Review Article

JCBFM

Journal of Cerebral Blood Flow & Metabolism
2016, Vol. 36(4) 647–664

DOI: 10.1177/0271678X15617954
jcbfm.sagepub.com

SAGE

Neurovascular coupling in humans: Physiology, methodological advances and clinical implications

Aaron A Phillips[1,2,3], Franco HN Chan[2], Mei Mu Zi Zheng[2,3], Andrei V Krassioukov[2,3,4,5,6] and Philip N Ainslie[1]

Abstract

Neurovascular coupling reflects the close temporal and regional linkage between neural activity and cerebral blood flow. Although providing mechanistic insight, our understanding of neurovascular coupling is largely limited to non-physiological *ex vivo* preparations and non-human models using sedatives/anesthetics with confounding cerebrovascular implications. Herein, with particular focus on humans, we review the present mechanistic understanding of neurovascular coupling and highlight current approaches to assess these responses and the application in health and disease. Moreover, we present new guidelines for standardizing the assessment of neurovascular coupling in humans. To improve the reliability of measurement and related interpretation, the utility of new automated software for neurovascular coupling is demonstrated, which provides the capacity for coalescing repetitive trials and time intervals into single contours and extracting numerous metrics (e.g., conductance and pulsatility, critical closing pressure, etc.) according to patterns of interest (e.g., peak/minimum response, time of response, etc.). This versatile software also permits the normalization of neurovascular coupling metrics to dynamic changes in arterial blood gases, potentially influencing the hyperemic response. It is hoped that these guidelines, combined with the newly developed and openly available software, will help to propel the understanding of neurovascular coupling in humans and also lead to improved clinical management of this critical physiological function.

Keywords

Automated software, cerebral blood flow, cerebrovascular, functional hyperemia, neuronal activation

Received 11 June 2015; Revised 22 October 2015; Accepted 23 October 2015

Introduction

The human brain comprises only 2% of body weight, yet consumes more than 20% of oxygen and glucose at rest, with almost all adenosine triphosphate in the brain being produced by oxidative metabolism of glucose.[1] In addition to a great need for substrate provision and by-product clearance, the metabolic circumstances in the brain are compromised by a limited intra-cellular capacity for energy storage. These two characteristics, combined with the paramount importance of brain function in comparison with other end-organs, create a situation where coupling of blood flow requires careful matching to changes in neuronal activation. The brain is well equipped to provide suitable blood flow for a given metabolic demand due to two components: extremely high vascularization, as well as redundant and sophisticated regulation of blood flow.[2] One primary factor responsible for

[1]Centre for Heart, Lung and Vascular Health, School of Health and Exercise Sciences, University of British Columbia – Okanagan, Kelowna, British Columbia, Canada
[2]International Collaboration on Repair Discoveries (ICORD), UBC, Vancouver, Canada
[3]Experimental Medicine Program, Faculty of Medicine, UBC, Vancouver, Canada
[4]Department of Physical Therapy, UBC, Vancouver, Canada
[5]GF Strong Rehabilitation Center, Vancouver, Canada
[6]Department of Medicine, Division of Physical Medicine and Rehabilitation, UBC, Vancouver, Canada

Corresponding author:
Aaron A Phillips, International Collaboration on Repair Discoveries (ICORD), University of British Columbia, 818 West 10th Avenue, Vancouver, BC, Canada V5Z1M9.
Email: aaphill@interchange.ubc.ca

ensuring appropriate blood supply within the brain is neurovascular coupling, which describes a close temporal and regional linkage between neural activity and cerebral blood flow (CBF) responses. This manuscript will review the major issues related to neurovascular coupling including: the anatomic structure of cerebral vasculature, organ-level mechanisms regulating CBF; provide insight into the mechanisms underlying the neurovascular response; outline the various methods used to measure neurovascular coupling in humans; present new guidelines for standardizing the assessment of neurovascular coupling in humans; and highlight the related alterations in neurovascular coupling in clinical conditions. Furthermore, this manuscript will describe a new analytical process to enable reliable and consistent assessments of human neurovascular coupling and provide directions for future research into this exciting and fascinating line of inquiry.

Anatomic structure

The internal carotid and vertebral arteries (ICA, VA), which branch off of the subclavian arteries, are the two conduit vessels providing blood delivery to the brain. The internal carotid arteries transmit approximately 70% of total CBF, while the remainder is provided by the VAs. In healthy individuals under typical scenarios, the VAs primarily provide blood flow to the brainstem, cerebellum, and occipital cortex. The VAs converge to form the basilar artery which then serves as a tributary to the circle of Willis and emerge as the posterior cerebral arteries. The circle of Willis is a crucially redundant anastomotic safety net evolutionarily commissioned to maintain perfusion if blood flow if one or more extracranial cerebral arteries is disrupted. It also represents the terminus of the internal carotid, which then contributes to the middle cerebral artery (MCA). The anterior cerebral arteries branch off the anterior aspect of the circle of Willis. The anterior, middle, and posterior cerebral arteries branch extensively before wrapping the brain surface in an array of vascularized tissue within the pia mater. Pial arteries then penetrate into the cortex. Upon penetration, arterioles are located within the Virchow-Robin space (i.e., pia mater protrudes into the brain with the arteriole). Once the arteries completely penetrate the parenchyma, they are considered ''parenchymal'' and are completely enveloped by astrocytic end-feet.[3]

Extracranial arteries (e.g. internal and vertebral arteries), large arteries of the brain (e.g. MCA), as well as pial arteries on the brain surface, are richly innervated by ''extrinsic'' perivascular postganglionic neurons from both sympathetic and parasympathetic origins.[4,5] On the other hand, parenchymal arterioles are regulated by ''intrinsic'' factors within the parenchyma, which are mediated by neuronal activation and astrocytic modulation.[6] Parenchymal arteries have greater basal tone and do not respond effectively to neurotransmitters, including norepinephrine and serotonin, which do elicit changes in the tone of upstream pial arteries.[6] All arteries in the brain contain a specialized endothelial layer, which functions as a barrier in an attempt to tightly regulate exchange between the blood supply and the brain (i.e., blood-brain barrier). In addition to this, tight junctions prevent paracellular passage and connect the innermost layer of epithelial cells.

Regulation of cerebral blood flow

Regulation of CBF is achieved through several factors including metabolic, myogenic, neurogenic, and systemic control.[7] Specifically, the primary controllers of CBF are partial pressure of arterial blood gases (CO_2 and O_2), cerebral metabolism, and the autonomic nervous system.[8,9] Under conditions of sufficient perfusion pressure, the remaining factors interact to regulate CBF by modulations in cerebrovascular resistance.[10] Cerebral blood flow is particularly sensitive to partial pressure of arterial CO_2, as reflected in a 1-mm Hg increase or decrease from eupnoeic CO_2 levels leading to a 3−6% elevation or a 1−3% reduction in CBF, respectively.

The large conduit arteries of the neck provide a large degree of influence in the regulation of CBF. Early canine *in situ* work showed that the arteries of the neck (i.e., ICA and VA) may provide as much as 50% of cerebrovascular resistance at rest.[11–13] These large arteries actively change diameters in response to various stimuli including alterations in arterial blood gas partial pressures,[14] and orthostatic challenges.[15] Both extracranial and pial arteries are innervated by sympathetic neurons originating from the superior cervical ganglion, which may serve to regulate CBF through the release of norepinephrine and neuropeptide Y.[4,16–19] Parasympathetic neurons from cranial nerves of the otic and pterygopalatine ganglia also modulate cerebrovascular tone by releasing acetylcholine, vasoactive intestinal peptide (VIP), and nitric oxide (NO), while the trigeminal ganglion fibres release a variety of other vasorelaxant mediators.[4,20] This is in contrast to the vast majority of systemic vasculature where the parasympathetic nervous system does not actively regulate tone. Despite extensive autonomic innervation in the brain, findings in humans support only a modest and somewhat frequency-dependent role of sympathetic[21–23] and parasympathetic activity[24] in influencing dynamic cerebral autoregulation. The details of the complex interactions involved in human CBF regulation have recently been reviewed.[9] The focus of this

article is on the relatively unexplored topic of neurovascular coupling in humans. Herein, particular focus will be made on the physiology and pathophysiology of neurovascular coupling, methodological limitations, and advances in this field.

Mechanisms of neurovascular coupling

The neurovascular unit is made up of three major components: (1) the vascular smooth muscle, (2) the neuron, and (3) the astrocyte glial cell (Figure 1). At a rudimentary level of detail, modulations in neuronal activity cause changes in local blood flow mediated by transmission through the astrocyte. This interaction is termed "neurovascular coupling," which describes coupling between neuronal activity and the vasculature. Tight temporal and amplitudinal linkage between neuronal activity and CBF delivery has been observed for >120 years.[25–27] There is much nuance and redundancy in this simplistic explanation of the neurovascular unit's interactions. For example, the neuron also alters vascular tone independently of astrocytic mediation, and these two cells play a synergistic or antagonistic role depending on the physiological environment. Readers are referred to recent reviews on this topic for further details.[2,28,29]

Both neurons and astrocytes respond to increased extracellular glutamate to transmit direct and indirect vasoactive signals for the appropriate delivery and distribution of CBF.[2] For example, glutamate released from presynaptic terminals activates N-methyl-D-aspartate receptors on neurons, which in the presence of sufficient intracellular oxygen and glucose, will stimulate the activation of neuronal NO synthase that provides NO to act directly on the parenchymal arterioles as a dilator.[30] Adenosine will also be directly

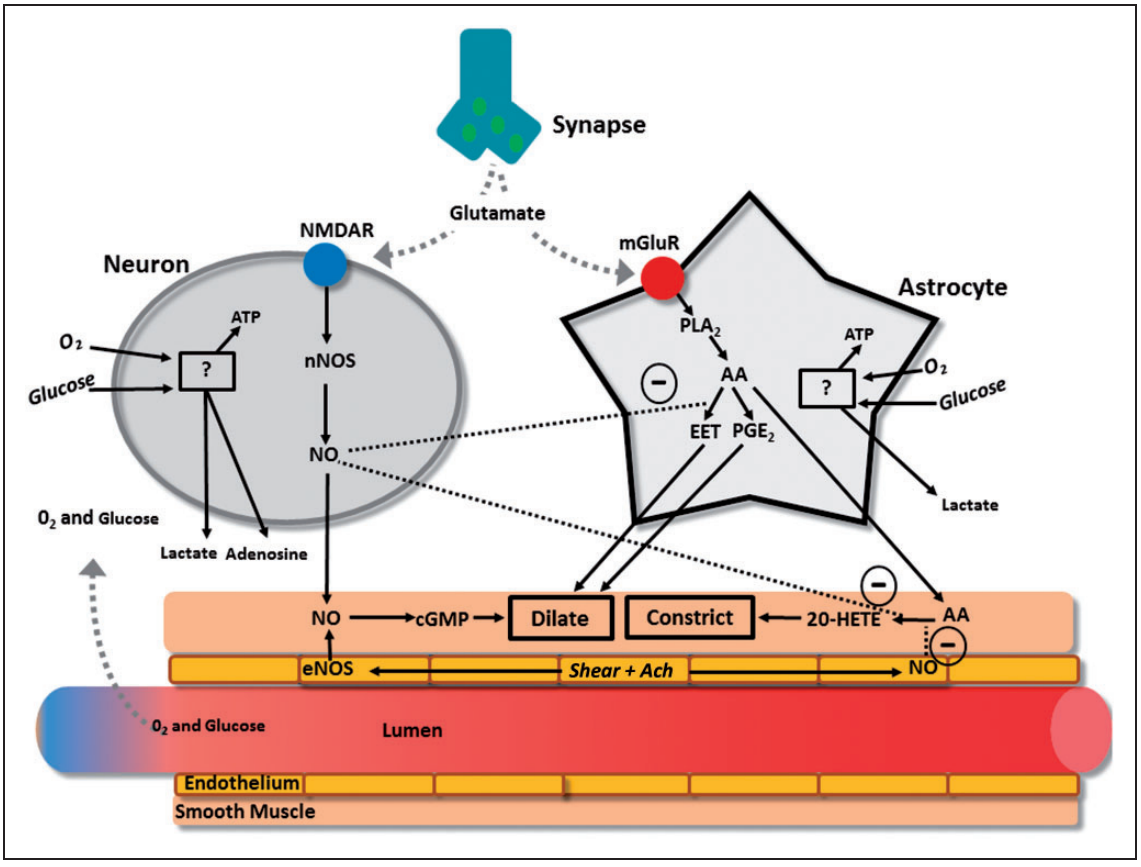

Figure 1. Primary glutaminergic pathways involved in cerebral blood flow regulation. Glutamate release by the synapse activates N-methyl-D-aspartate receptors (NMDAR) on neurons as well as metabotropic glutamate receptors (mGluR) on astrocytes. Both of these receptors act by increasing cytosolic calcium concentration. In the neuron, Ca2+ activated neuronal nitric oxide synthase (nNOS) produces nitric oxide (NO). Increases in Ca2+ within the astrocytes activate phospholipase A2 (PLA2), which generates arachodonic acid (AA), and therefore both epoxyeicosatrienoic acid (EET) and prostaglandin E2 (PGE2), both of which dilate cerebral arteries.[128–130] Nitric oxide exerts diverse effects including: 1) activating cyclic guanosine monophosphate (cGMP) in smooth muscle leading to dilation,[131] 2) inhibiting 20-hydroxyeicosatetraenoic acid (20-HETE) in smooth muscle to inhibit constriction,[132,133] and 3) inhibiting production of EET in astrocytes which inhibits the vasodilatory action of EET on smooth muscle.[129]

released to act as a vasodilator when neuronal adenosine triphosphate is low.[31] Similarly to neurons, astrocytes respond to glutamate through metabotropic glutamate receptors, which again in the presence of sufficient intracellular oxygen and glucose, activate a cascading pathway involving the production of arachidonic acid which then produces epoxyeicosatrienoic acid and prostaglandins.[32] Both prostaglandin and EET serve to dilate parenchymal arterioles, while arachidonic acid, after diffusing out of the astrocytes and into the smooth muscle, produces vasoconstriction.[33] There also appears to be a complex relationship between astrocytes, incoming neuronal signals, and GABA interneurons that are thought to play a local integrating role precisely regulating local CBF delivery.[29,34,35] These interneurons are ideally placed between glutaminergic pyramidal cells and project onto microvessels.[35,36] Indeed, evoked firing of GABA interneurons resulted in increased concentration of a variety of vasoactive substances (e.g., NO, acetylcholine, neuropeptide-Y, VIP) that led to both constriction and dilation of cerebral microvasculature.[34,35]

Under normal conditions, the double stimuli (i.e., neuronal and astrocytic) leads to a 4-fold greater increase in CBF relative to the increase in ATP consumption.[37] This overcompensation of functional hyperemia appears to support the feed-forward mechanism.[37] It should be noted however that a feed-backward system capable of functional hyperemia has also been proposed as a compensatory mechanism in a model incorporating capillary transit time heterogeneity, maximum oxygen extraction fraction, metabolic rate of oxygen and CBF.[38] Together, these factors demonstrated that more homogenous capillary flow and exaggerated CBF response compensated for reduced oxygen extraction during functional hyperemia.[38] This overabundance of blood flow relative to metabolism is the theoretical foundation of blood-oxygen level dependent (BOLD) magnetic resonance imaging; which relies on the assumption that increases in deoxygenated blood are associated with increased neuronal activity.[39]

Although astrocytes are sufficient to evoke a neurovascular coupling response, it is unclear whether astrocytes are necessary for functional hyperemia to occur.[40,41] Recently, it has been proffered that the role of astrocytes during neurovascular coupling is isolated to maintaining blood flow suitable for basal neuronal activity and to producing a ''slow-onset'' hyperemia (i.e., 3–4 s post neuronal activation) but not to be active in the immediate hyperemic effect that occurs in <1 s.[41] Recent and sophisticated assessments of the neurovascular coupling response to visual stimulation showed that astrocytic endfeet/Ca2+ signalling was not responsible for the rapid functional hyperemia;[40] readers are referred to more in-depth reviews on this topic.[28,42] This is a somewhat emerging but compelling contention, such that it deserves mention in the context of the present review.

It is not just the arteriole smooth muscle that regulates neurovascular coupling, although this has been the primary understanding until very recently. Pericytes (i.e., small cells expressing contractile tissue located at 50 μm intervals along the length of capillaries)[43] likely also play a large role in neurovascular regulation, as suggested by their anatomic arrangement.[44] For example, neurons are more often closer to pericytes than arterioles, creating the plausible scenario whereby neuronal activation first alters resistance through modulations in pericyte tone on capillaries, and signals are then transmitted 'up-stream' to arterioles.[45] Pericytes are theorized to be regulated in much the same way as arterioles.[44] Brain slice preparations show that glutamate and norepinephrine lead to dilation and constriction of pericytes, respectively, and blocking glutaminergic receptors leads to vasoconstriction.[46] The intervals between pericytes necessitate the transmission of vasoactive signals through gap junctions; however, whether these travel between pericytes/endothelial gaps remains to be elucidated.[44,46] In any case, there is a huge capacity for the pericytes to influence neurovascular coupling. For example, it has been modelled that anywhere from 16–70% of resistance within the brain parenchyma is produced by capillaries.[47,48] In reality this may be even larger, as capillaries are so narrow that white and red blood cells have to deform to pass through, creating even more resistance than Poiseuille's law predicts.[49]

The combination of incongruent findings,[40,50] the elucidation of highly redundant mechanistic pathways,[41] and limited translational capacity has led to the acknowledgment that the mechanisms of neurovascular coupling need to be better explored *in vivo*/human models rather than just in animals and isolated well-controlled preparations (e.g., two-photon imaging, brain slices, etc.).[41,51] Establishing a standardized protocol for evaluating human neurovascular coupling *in vivo* would allow for insight into not only the mechanisms underlying this fundamental response but also how neurovascular coupling is altered in diverse populations (e.g., clinical populations, aging, etc.).

Human neurovascular coupling

Our present understanding of neurovascular coupling in humans is limited, and the available knowledge is generated from a small number of laboratories, using a variety of unstandardized assessments.[52–63] Although there is mechanistic insight provided by the isolated preparations of neurovascular coupling,[41] little is known about which mechanisms are sufficient versus

necessary for a functional and effective neurovascular coupling response in humans. The available literature related to this topic is reviewed below.

Data indicate that the neurovascular coupling response is comprised of highly redundant mechanistic regulation and is well maintained under a variety of physiological and pharmacological stressors. Such mechanisms are largely unexplored in humans to date. Recently, we have attempted to specifically antagonize cerebrovascular L-type calcium channels using nimodipine, which theoretically blunts the capacity for the cerebrovasculature to respond to an array of vasoactive mediators thought to play a role in neurovascular coupling from isolated preparations (i.e., bradykinin, vasopressin, dopamine, epinephrine, norepinephrine, histamine, glutamate, acetylcholine, serotonin, and prostaglandin).[64] Even with a clinically relevant dose of 60 mg, which is used to treat vasospasm, the neurovascular coupling response was normal as compared to a placebo control trial.[64] Although impaired in various pathologies (as described in detail below), neurovascular coupling is also maintained during exercise when a number of physiological parameters a significantly altered.[55] Together, these data indicate that human neurovascular coupling is remarkably robust and demonstrate the inability of isolated models to predict *in vivo* responses.

Outside of using physiological and pharmacological stressors, another approach to provide insight into the mechanisms underlying neurovascular coupling has been to use mathematical dynamic multivariate/autoregressive modelling.[54] Through subcomponent modelling, alterations in critical closing pressure (i.e., the pressure inside a blood vessel below which the vessel will collapse) and resistance area product (i.e., resistance with acknowledgement of unknown vessel diameter; inverse slope of instantaneous beat-by-beat relationship between CBF velocity and blood pressure) during neurovascular coupling are thought to provide selective indices of metabolic and myogenic cerebrovascular regulation, respectively, while the influence of blood pressure and changes in end-tidal partial pressure CO_2 ($ETCO_2$) on neurovascular coupling are also modelled.[65–67] Using this approach, a number of interesting studies have been completed with the following conclusions: (1) hypercapnia impairs the metabolic regulation of neurovascular coupling, (2) breath-by-breath changes in $ETCO_2$ during cognition can impact the neurovascular coupling response, and (3) the blood pressure response to cognitive activation plays a large role in the neurovascular coupling response, particularly the initial spike.[53,66,68] These interesting studies have yet to confirm a direct mechanistic link between the physiological regulatory pathways of interest (i.e., metabolic versus myogenic influences) and the subcomponent models/metrics being utilized (i.e. critical closing pressure versus resistance area product).

Some insight into neurovascular coupling in humans has been provided by unique models measuring concurrent cerebral tissue oxygenation and CBF. Although technically and environmentally challenging, these studies can provide detailed insight into flow-metabolism coupling. For example, using functional MRI, it is now known that a consistent BOLD signal over childhood development is underpinned by decreasing neuronal activation/metabolism counterbalanced by increasing neurovascular coupling.[39] Also when using this approach in the healthy human brain, oxygenated venous blood rises (i.e., increased BOLD signal) to a greater extent than CBF during visual stimulation, indicating the effect of exaggerated hyperemia beyond cerebral metabolic demand.[69] Furthermore, although reduced neural activity to a given stimulus has been reported after ischemic stroke,[70] a recent study combining BOLD, fluid attenuation inversion recovery, and arterial spin labelling has shown a variety of neurovascular coupling phenotypes in this population.[69] For example, individuals with ischemic stroke can exhibit a blunted, exaggerated or reduced functional MRI BOLD signal during visual stimulation, with exaggerated or blunted hyperemia.[69] Although these data indicate a mismatch between CBF delivery and oxygenation extraction/metabolism,[69] the mechanisms explaining the variability in the functional MRI BOLD signal responses during visual stimulation are unknown.

Clinical implications

Despite inconsistent methodologies, a number of studies have characterized neurovascular coupling in a variety of models of clinical conditions (and in some cases human populations), as summarized in Table 1. These conditions likely impact neurovascular coupling through a variety of diverse mechanistic pathways. For example, one fundamental factor underlying impairments of neurovascular coupling in clinical populations (i.e. high level spinal cord injury, autonomic dysfunction, and generalised hypotension) is the insufficient cerebral perfusion pressure, which likely renders any reductions in cerebrovascular tone secondary to neuronal activation futile for producing hyperemia.[52,71–73] On the other hand, conditions such as stroke and traumatic brain injury are likely impaired due to alterations in hyperemic signalling from glutamate release secondary to neuronal death and astrocyte scarring.[67,74–78] Furthermore, oxidative stress is suspected to play a particularly deleterious role in human neurovascular coupling and is implicated in the declines seen in hypertension (through angiotensin receptor type 1 agonism), Alzheimer's (through amyloid β accretion), diabetes (through chronic hyperglycemia),

and healthy aging (Table 1). It may be that reducing oxidative stress is a viable therapeutic target for improving neurovascular coupling in humans, although this possibility needs to be clearly examined.

An interesting relationship between cognitive activation and neurovascular coupling in humans has been demonstrated,[79] which provides a mechanistic link in conditions where cognition is impaired (Table 1). For example, chronic hypotension depresses cognitive activity and resting CBF, which is directly mediated by neurovascular coupling.[72,80] Conversely, cognitive activity can be improved with pharmacological treatment of hypotension, through improvements in neurovascular coupling;[52,81] demonstrating that cognitive function is positively related to neuronal tissue oxygen delivery. This link between impaired neurovascular coupling and cognitive decline needs to be further established in other clinical conditions, but if confirmed, may be particularly alarming in the smoking population, where neurovascular coupling does not normalize after cessation.[82] In order to increase the clinical utility of neurovascular coupling as an end-point treatment target, there is a need for an automated and standardized protocol for analysis, which produces interpretable metrics.

Finally, although not a feasible technique in most scenarios, treatment of traumatic brain injury (where the brain is exposed) can allow for direct measurement of CBF, local metabolism (via microdialysis) and/or oxygenation across brain tissue.[83] Under these conditions, it has been demonstrated that during cortical spreading depolarization, the neurovascular coupling response often becomes inverse with neuronal activation, leading to a hypo-emic response.[77] The mechanisms underlying this inversion are unknown; however, this response likely further compromises survival of cerebral tissue which is already ischemic. Clearly, a plethora of future studies are required to delineate the major factors and redundancies in the human *in vivo* neurovascular coupling response.

Assessing neurovascular coupling in humans

In the following sections, we will illustrate how transcranial Doppler (TCD) and/or near-infrared spectroscopy (NIRS) approaches are used for neurovascular coupling evaluation in humans and describe a standardized approach for eliciting the neurovascular coupling

Table 1. Neurovascular coupling in various clinical conditions.

Pathology	Impact on neurovascular coupling	Mechanism
Stroke	Impaired – particularly in hemisphere of insult	Brain edema, inflammation, impaired neurotransmission, and neuronal death impairs normal neuronal activation.[a] Also, activation of non-specific brain structures further complicates interpretation. [67,74,75]
Hypertension	Impaired	Elevated circulating angiotensin II leads to: 1) activation of AT1 receptors on cerebral blood vessels, 2) increased oxidative stress which inhibits neuronal and astrocytic vascular dilators.[a,134,135]
Hypotension	Impaired	Inadequate perfusion pressure inhibits efficacious hyperemic response, although neuronal signalling may be normal.[52]
Autonomic Dysfunction	Impaired	Impaired blood pressure responses, as well as altered neurogenic regulation of neurovascular coupling.[b,52,73]
High level spinal cord injury	Impaired	Unknown.[b] Persistent dysfunction of neurovascular coupling after restoring normal blood pressure.[52]
Traumatic Brain Injury	Impaired	Neuronal death and astrocytic scar formation precludes normal neurovascular response.[a,76–78]
Alzheimer's	Impaired neurovascular coupling and impaired resting cerebral perfusion.	Hypercontractility (phenylephrine) of smooth muscle, increased basal and enhanced occurrence of spontaneous Ca2+ waves.[a] Amyloid Beta also directly inhibits functional hyperemia by promoting oxidative stress which inhibits neuronal and astrocytic vascular dilators. [136–138]
Smoking	Impaired	Unclear – but does not appear to reverse after cessation: indicating long term alterations in structure/function of the neurovascular unit.[b,82]
Diabetes	Impaired	Impaired astrocyte function due to high circulating glucose and increased oxidative stress.[a] Prolonged hyperglycemia interferes with astrocytic gap junctional communication.[139,140]
Healthy Aging	Impaired	Reduced with healthy aging,[59] however exercise may be viable intervention to slow the decline.[b,141] Dynamic lateralization of cerebral blood flow may also be impaired with health aging.[142]

[a]Mechanistic insight provided only by animal models/isolated preparations. [b]Mechanisms not clearly established.

response. Furthermore, we will outline a suggested standardized protocol for neurovascular coupling evaluation, description and quantification in humans, which employs newly developed automated software.

Transcranial Doppler

In humans, the most commonly used approach to study neurovascular coupling involves the use of transcranial Doppler (TCD). The high temporal resolution and non-invasive nature of TCD make it a useful tool in the assessment of integrative cerebrovascular function in terms of neurovascular coupling. New technologies further increase the utility of TCD. A TCD machine is relatively inexpensive ($25,000–$50,000 USD); moreover, TCD is easy to use and is safe in healthy and disease states alike. Therefore, it is practical to use TCD in the clinical setting to assess a variety of different cerebrovascular pathologies. Although the diameter of major arteries may change with fluctuations in arterial blood gases,[14,84] the range of arterial CO_2 at which TCD accurately estimates changes in CBF is not exceeded during standard neurovascular coupling protocols.[52,67] The functional anatomy of the brain allows neurovascular coupling to be easily and reliably examined by measurement of the sensorimotor or cognitive stimulatory effects on cerebral blood velocity; a method termed functional TCD. This technique was first utilized by Aaslid in 1987, who showed that blood velocity in the posterior cerebral artery (PCA) changed with visual stimulation (Figure 2),[85] but there are numerous studies in the neuro-cognitive literature that demonstrate consistent CBF changes in response to cognitive, verbal and motor tasks.[85–88] In healthy individuals, this response will lead to an average of 10−20% increase in CBF in the PCA and a 5−8% increase in the MCA (Figures 2 and 3).[59,86,89] Further, our group and others have explored hemispheric lateralization of CBF delivery using either right-handed/verbal tasks or left-handed motor paradigms to preferentially activate the left and right MCA.[66,90] This latter technique has shown that indeed verbal-tasks combined with right-handed motor function lead to hyperemia preferentially in the left hemisphere, while spatial-tasks combined with left-handed motor function lead to hyperemia preferentially in the right hemisphere (Figure 4).[66,90]

Detailed instructions on insonating the MCA and PCA have been provided elsewhere.[91] Briefly, MCA blood velocity is generally viewed at 35−60 mm depth, after placing the Doppler probe on the middle transtemporal window oriented in line with the coronal axis. The PCA can then be viewed most commonly at 60−70 mm using the anterior transtemporal window by tilting the Doppler probe slightly posteriorly from the MCA. The P1 segment of the PCA will result in blood flow toward the Doppler probe, while the P2 segment curves away from the probe. Both the P1 and P2 segments have been utilized with similar results, however a consistent segment should be maintained throughout a given study.[52,55,73,92,93] Lastly, often only the posterior window is suitable for insonating intracranial vessels in the elderly, due to skull thickening with advancing age.[94] Some studies have reported that 10−15% of

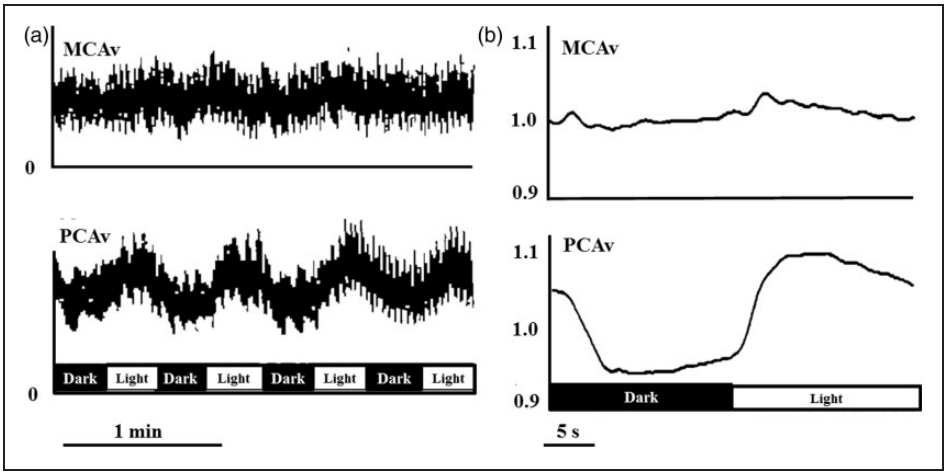

Figure 2. Traditionally reported hyperemia of the visual cortex to light stimulation in humans. (a) Middle cerebral artery blood velocity (MCAv), and posterior cerebral artery blood velocity (PCAv) during repetitive cycles of light exposure and darkness to the retina. Data is presented as relative changes. (b) Average responses to at least 16 repetitive dark and light sequences from each of 10 normal individuals for MCAv and PCAv. Figure adapted from Aaslid.[85]

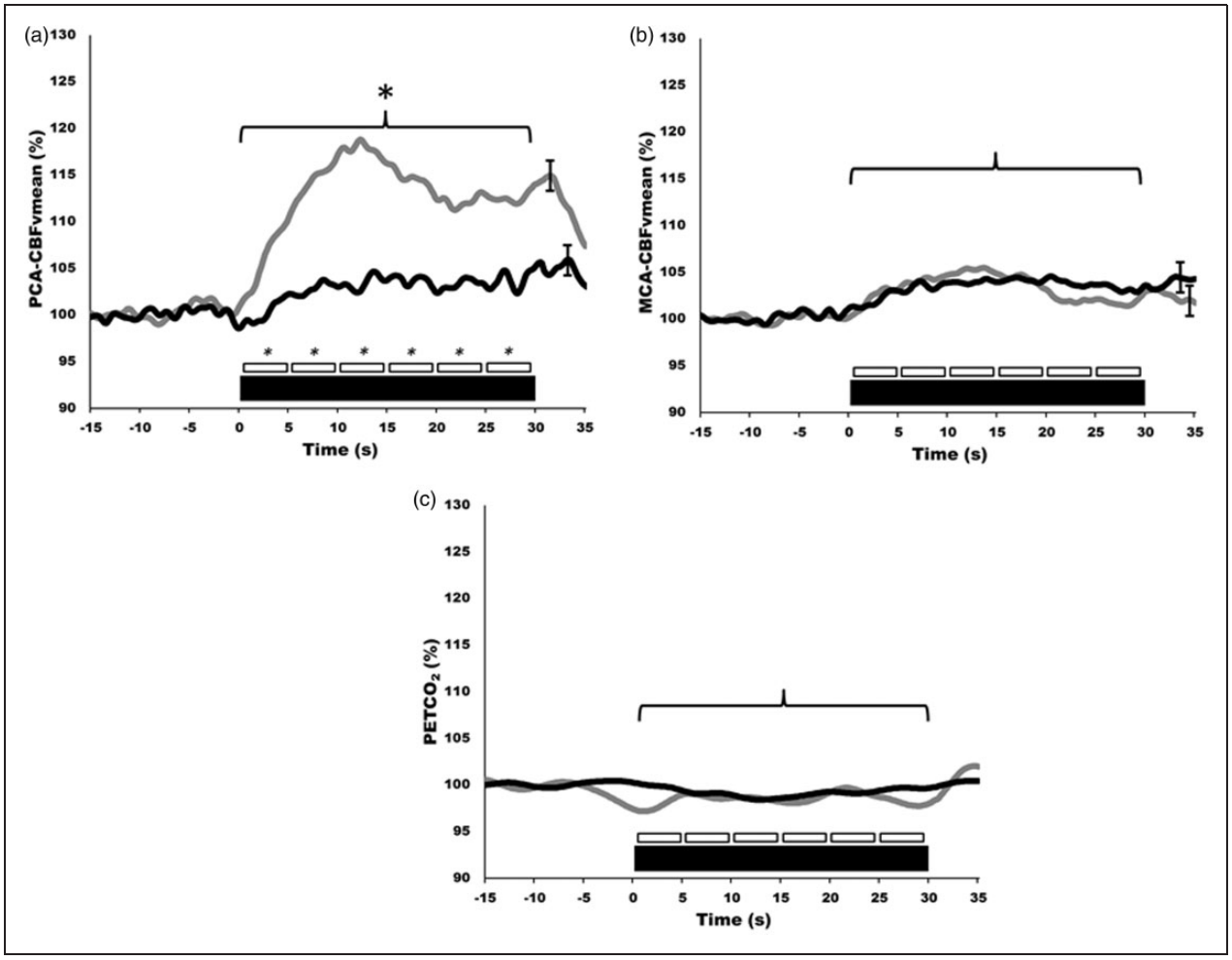

Figure 3. Neurovascular coupling in humans generated from automated software using established standardized eyes-open/eyes-closed protocol. (a–c) Hyperemic responses, during visual stimulation, of the posterior cerebral artery (PCA; a), middle cerebral artery (MCA; b), and partial pressure end-tidal carbon dioxide ($PETCO_2$; c). Note the selective activation of the PCA of around 20% vs. just 4−5% in MCA. Grey lines indicate healthy control group, black bars indicate high-level spinal cord injured group. Thick black bar indicates 30 s of eyes-open reading, being immediately preceded by eyes-closed. Smaller boxes represent 5 s bins which were averaged and compared quantitatively. These contours represent the response of 10 trials for each of 10 participants.

individuals will have inadequate windows for insonating intracranial cerebral vessels;[95] as such, it may be advantageous to utilize other techniques such as NIRS (see next section) in addition to TCD for studies in the elderly or those with related cerebrovascular pathology.

It is now clear that the diameter of the MCA (and hence possibly the PCA) is influenced by marked changes in arterial PCO_2 (>8 mmHg above or below resting) and arterial PO_2 (<50 mmHg)[84,96] (reviewed in literature[9,97]). It is less clear that changes in blood pressure will affect the diameter of these intra-cranial arteries. However, it would seem highly unlikely that hyperemic responses noted in the MCA/PCA are being affected by changes in arterial diameter over the neurovascular coupling response. The major reason is that changes in vasoactive influencers (i.e., arterial blood gases) do not occur and the NVC response is very rapid (~1 s). For example, no discernable change in $PETCO_2$ has been noted during 30−60 s of stimulation. [52,98] Furthermore, if the diameter of the MCA (or PCA) was dilating during the NVC response and being directly impacted by metabolic demand/hypoxia, this would be reflected in a blunted or absent hyperemic response (i.e., the dilation of the MCA/PCA would lead to a reduction in blood velocity). Thus, the major site driving the NVC response seems to be the neurovascular unit rather than the larger intracranial arteries.

Near infrared spectroscopy

In addition to TCD, NIRS can also be used for assessing neurovascular coupling in humans.[99–102] Incorporating NIRS can indirectly quantify changes in oxygenated and

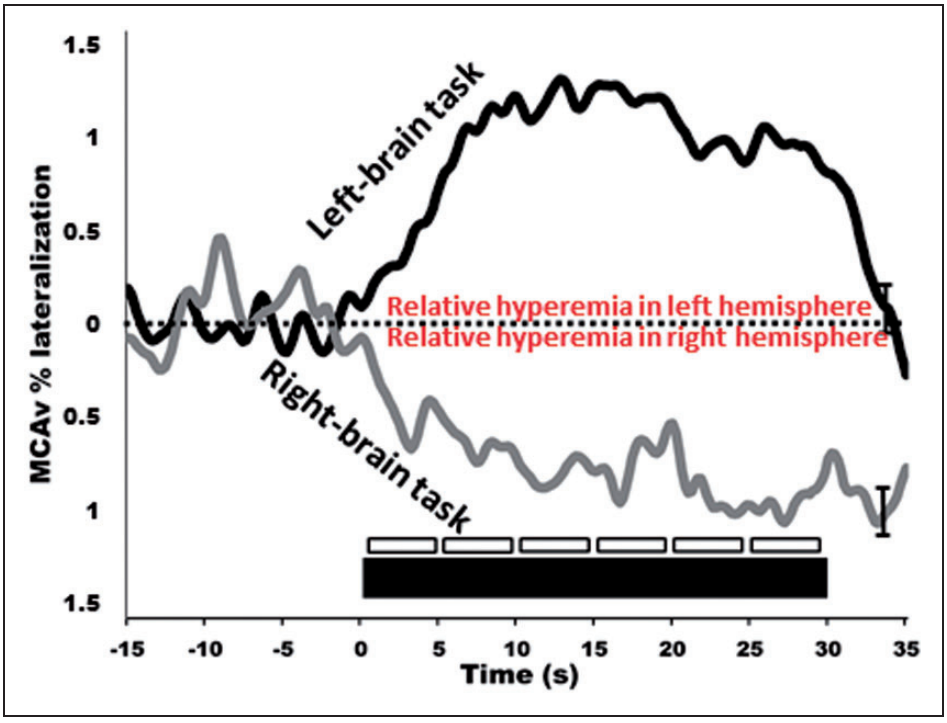

Figure 4. Dynamic lateralization of hyperemic responses. In healthy individuals left-brain tasks lead to selective hyperemia of the left MCA, and the opposite occurs for right-brain tasks. The left-brain task involved using the right-hand to complete a verbal fluency test, whereas the right-brain task involved using the left-hand to build presented two-dimensional images as three-dimensional structures. Thick black bar indicates 30 s of left/right-brain activation preceded by eyes-closed. Smaller boxes represent 5 s bins which were averaged and compared quantitatively. These contours represent the response of 10 trials for each of 10 participants.

deoxygenated hemoglobin, based on the relative transparency of tissue to near-infrared light, and oxygen-dependent light absorption caused by hemoglobin chromophores. As such, both quantitative and regional indexes of CBF can be provided utilizing the blood-oxygen level dependent signal to detect changes in oxygenated (O_2Hb), deoxygenated, (HHb) and total hemoglobin (tHb) within for the most part, the venous vessels of the brain (i.e. $<$1 mm).[103] Like the TCD, NIRS has very high temporal resolution and can most commonly provide analog outputs at $>$20 Hz. Moreover, NIRS is also similar to TCD in terms of cost and ease of use. As NIRS also provides some insight into changes in CBF, the underlying arterial CO_2 must be considered, as alterations will affect CBF independently from changes in neuronal activity.[104] Also similar to TCD, NIRS can evaluate CBF responses to neuronal activation using a variety of strategies of activation including various emotional, sensory, motor, and pure cognitive tasks.[105,106] The history of the development of NIRS is well documented (reviewed in the literature[103]). The NIRS response during NVC is similar to that generated using TCD and typically results in increased O_2Hb and tHb with a concurrent small decrease in HHb; these responses are similarly regionally specific (i.e., visual stimulation leads to posterior cortex hyperemia).[99] During repeated squat-stand maneuvers where blood pressure rapidly increases and decreases, changes in NIRS and TCD were of similar amplitude however changes in NIRS signals trailed those from TCD by 1.8–2.6 s, which may be the result of arterial transit time and fundamental differences in anatomic location between TCD and NIRS.[107] Further, when using other vasoactive stimuli, such as hypercapnia, the NIRS-derived percent hyperemic response is markedly less (1–15% increases vs. 20–100% increases) of that demonstrated by NIRS.[108] This discrepancy, likely reflecting different physiological mechanisms, potentially impacts the sensitivity of NIRS to detect significant differences between clinical and control populations.[109] Clearly, more studies are needed to address the congruency of TCD and NIRS signals during NVC. Care must be taken to ensure that the optodes are located in appropriate locations of the participant's head to allow for the evaluation of hyperemic responses in relevant portions of the brain, and that the sources and detectors are appropriately spaced. These guidelines are somewhat less stringent as compared to TCD and involve placing the optodes over the general area of interest (i.e., posterior cortex, frontal, partietal lobe, etc.).[99] Apart from the frontal cortex, however, hair will impede signal quality in other brain regions unless the hair is removed.

Nevertheless, the simultaneous assessment of TCD (as an index of blood flow delivery) with NIRS (as an index of cerebral tissue oxygenation, the key end-point of interest for neuronal viability) during NVC will provide complimentary insight into integrated cerebrovascular physiology and will permit the inclusion of more subjects, especially when TCD is not possible.

Although TCD and NIRS are by far the most widely used tools for neurovascular coupling measurement in humans, there still exists significant variability in the software and strategies used to analyze these metrics. For example, many studies simply report the maximal change in CBF recorded during the "activation" period with[55,92,110] or without[111,112] addressing the temporal characteristics, while others attribute specific components and characteristics of the hyperemic contour to specific influences (i.e., perfusion pressure, neurogenic, autoregulation, blood gas concentration).[54,74] Our approach is to incorporate both amplitudinal and temporal characteristics by plotting the entire hyperemic contour, while extracting data from temporal subdivisions (i.e., early versus late/5 s duration bins, etc.) for further analysis.[52] The amount of data analysis required for the latter two approaches is significant, with a variety of processing steps required to coalesce contours into interpretable metrics.

Eliciting the neurovascular coupling response

A robust neurovascular coupling response can be assessed by simple visual stimulation (i.e., opening eyes/reading) during beat-by-beat measurement of blood flow/velocity in the PCA relative to the MCA, the prior of which is associated with perfusion of the visual cortex.[52] The selective activation of the occipital lobe is achieved using repeatable and reliable stimuli involving an eyes-open task against a bright visual stimuli (reading, flashing screen, eyes tracking tester's moving hand, etc.). The visual stimulation provides a strong mechanistic model of neurovascular coupling that is somewhat independent of variable neuronal activation schemes (i.e., a variety of different visual spatial tasks elicit similar PCA hyperemic responses);[73] however, less is understood about the hyperemia response in MCA or anterior cerebral arteries to tasks of varying difficulties or under different states of motivation. Conventionally, after a 10–15 min period of quiet rest (to allow stabilization of blood volume and hemodynamic signals), 5–10 cycles are repeated where each cycle consists of a 20–30 s period of eyes-closed time followed by 30–40 s of eyes-open time.[52,73] The greater the number of cycles, the higher the signal-to-noise ratio; however, this obviously must be balanced with the time constraints of the study and the impact on the participants whom may be from a clinical population. Patient positioning can vary depending on study design. Often for clinical relevance, the seated position is used; however, participants may be positioned supine if studying different loading conditions. Similarly, the left or right PCA can be chosen while assessing the contralateral MCA, although this must be consistent throughout the study as perfusion properties can vary between the left and right sides and often CBF is elevated to the left hemisphere.[113]

All testing should take place in a quiet, temperature-controlled and well-lit room. Depending on the study design, participants should avoid alcohol, caffeine, and strenuous exercise at least 12 h prior to testing, and be fasted for at least 4 h as these factors can influence vascular tone and function.[114–125] Furthermore, assessments should take place at the same time of day, and in the same menstrual phase for premenopausal women.[115] Additionally, medications should be avoided for at least four half-lives if possible, whereas non-steroidal anti-inflammatories should be discontinued for 2–3 days.[126,127] This latter recommendation may be problematic in many clinical conditions; however, in any case, all medications should be carefully documented and considered during data interpretation. Due to the ease of administering the test, if artifact occurs within a cycle, another cycle should be added and used to replace the aberrant cycle. If a trial with an artifact needs to be included, the problematic data points should be linearly interpolated using one data point on either side of aberrant data. If more than two aberrant data points occur, this cycle should be removed. Please see Figure 5 for a detailed description of proposed standardization protocol.

Analysis considerations

Hemodynamic data from each original hyperemic recording are extracted on a beat-by-beat basis using a variety of acquisition systems available (i.e., LabChart, LabView, etc.). The required outputs from the data acquisition programs include RR interval, systolic, diastolic, and mean arterial pressure as well as mean, peak and minimum velocity from the TCD/NIRS. After extraction, data from each subject and condition are placed in a separate spreadsheet that includes all of the 5–10 repeated neurovascular coupling cycles collected. After this, the software automatically coalescences all trials from that participant into one contour for each outcome metric of interest (see Table 2) over the "eyes-closed" and "eyes-open" period. From this average response within a participant, metrics over a fully adjustable range of "bin" durations (i.e., 1 s, 5 s, 10 s, etc.) can be extracted for statistical analysis (see Table 2). Finally, a single group-averaged (± standard error/deviation) contour at a

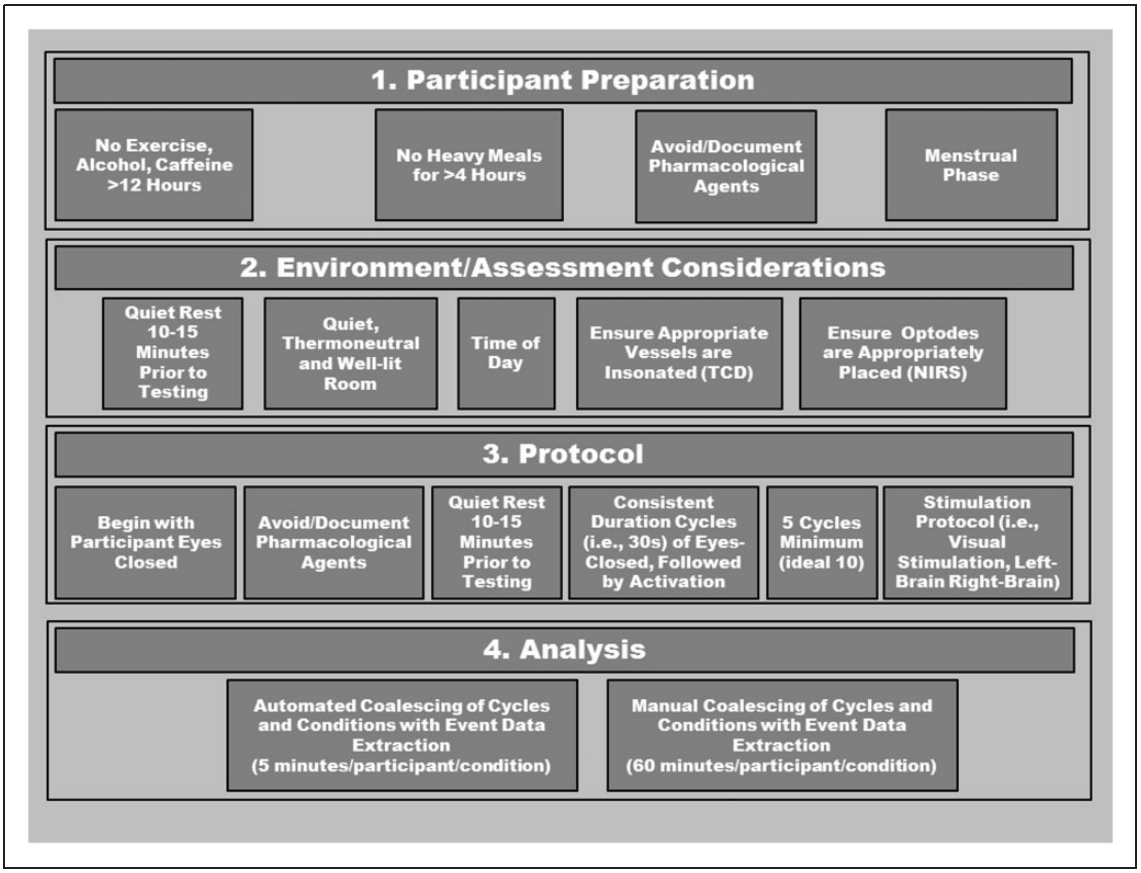

Figure 5. Recommendations for the assessment of neurovascular coupling in humans using transcranial Doppler (TCD) or near-infrared spectroscopy (NIRS). After ensuring appropriate participant preparation, testing should take place in a suitable environment with confidence that vessels/brain regions are accurately detected. Testing should also take place at consistent time of day between participants and conditions. A 10–15 min period of quiet rest in the testing position should precede the actual testing, allowing for stable hemodynamics. The protocol itself should begin with the participants' eyes closed, and consist of 5–10 repeated cycles of 30 s eyes-closed, followed by eyes-open, followed by eyes-closed, with no time between. The timing of the cycles should be precise, and the assessor should ensure initiation of the "task" (i.e., eyes-open, closed, cognitive task) is immediate. Manual analysis can be extremely time-consuming; however, automated analysis is now available.

5 Hz sampling frequency is output for production in graphing software of the users' choice for any of the above metrics (Table 1, Figure 3). End-tidal gases are extracted on breath-by-breath basis and are also interpolated at 5 Hz and can be used to normalize CBF metrics for changes/differences in arterial blood gases. These data are then plotted identically.

In order to normalize the time-scale to when heart/breathing rates are different between subjects/trials or within trials (which is critical when input values are sampled at different frequencies (i.e., heart rate and breathing frequency)), y-axis data are cubic spline interpolated and re-sampled in the x-axis at 5 Hz. As opposed to linear interpolation, which resamples data from a constructed straight line between data points, the cubic spline function has contributions from second derivative and degree-3 polynomial pieces that together allow for prediction of data points transitioning between extracted data points. Due to increased accuracy, a cubic spline interpolation likely provides more physiologically relevant transitions between data points.

Future directions

In an attempt to propagate our understanding of neurovascular coupling in humans, we have taken the step of developing standardized and automated software for neurovascular coupling analysis. Using the high temporal resolution of TCD or NIRS, this program automatically detects and coalesces multiple trials within participants and generates a hyperemia contour for each condition (see Figure 3). Furthermore, this software extracts a vast array of metrics for statistical analysis between groups and/or conditions (Table 2). Moreover, this software generates group mean

Table 2. List of metrics and binning options available with current software.

Vessels	Measurement Techniques	Outcome metrics	Formula	Theoretic physiology associated with outcome metrics
ACA	TCD	vmax		
MCA	Beat-by-beat blood pressure[a]	vmin		
PCA		vmean	(2x(vmin) + (vmax))/3	
VA		CVC	vmean/MAP	Cerebral blood flow for given cerebral perfusion pressure indicates the ease of blood flow through the brain. With increasing vascular tone, conductance decreases. Because of the reciprocal relationship between conductance and resistance, it is recommended to use conductance in high flow situations, where resistance vessels are relatively relaxed, and modulations in tone lead to very little change in resistance but large changes in conductance. Due to this, if using CVR instead of CVC, the CVR response could be underestimating the decrease in tone during the increase in flow, as further increases in flow above the resting state may not result in a concomitant reduction in resistance although conductance is substantially increasing.[143,144]
ICA		CVR	MAP/vmean	Cerebral perfusion pressure for a given cerebral blood flow indicates the resistive forces acting on blood flow through the brain. With increasing vascular tone, resistance increases. [143,144]
		RAP	(SBP-DBP)/(vmean-vmin)	The instantaneous (i.e., over a single heart beat) theoretical relationship between blood pressure and flow. Indicates the change in perfusion pressure for a given change in cerebral blood flow. Describes how much perfusion pressure increases or decreases for a given change in cerebral blood flow. [145,146]
		CCP	MAP − (vmean × RAP)	The instantaneous (i.e., over a single heart beat) theoretical perfusion pressure at which cerebral blood flow ceases (i.e., becomes zero). Generally calculated as the pressure corresponding to zero cerebral blood flow when calculating the instantaneous relationship between blood pressure and cerebral blood flow. This value is generally above zero due to significant collapsing forces exerted on the vasculature from intracranial pressure and tension within the vessel walls themselves. [145–147]
		PI	(vmax-vmin)/vmean	Ratio of cerebral pulsatile blood flow to average cerebral blood flow. This is considered to be related to small cerebral vessel elasticity and tone. As small vessel tone increases, there is reduction in vmean resulting in increased PI; whereas as when vessels dilate, vmean increases resulting in a low PI. [148]
		PR	((vmax-vmin)/mean)/ ((SBP-DBP)/MAP)	Cerebral pulsatility index normalized for systemic pulsatility. It may not be appropriate to examine PI alone to represent cerebral small vessel tone, as a primary influence on PI is the systemic pulsatility coming into the cerebrovasculature. [149]
		T-Max/Min	Time of peak/min values	Unknown. Time of peak is calculated for all of the above metrics. As such, it likely provides insight into 'speed' of the NVC response.
		Lateralization	Leftvmean/ (Leftvmean + Rvmean) × 100	Relative hyperemic responses between hemispheres. vmean is used here as an example;, however, the percent lateralization is calculated for any of the above metrics.

Note: All variables can be calculated normalized to breath-by-breathe changes in $PaCO_2$/$ETCO_2$, and presented as absolute or percent changes. Furthermore, all values can be extracted from any time segment of interest (i.e., 5/15 s "bins"). ACA, anterior cerebral artery; MCA, middle cerebral artery; PCA, posterior cerebral artery; VA, vertebral artery; ICA, internal carotid artery; TCD, transcranial Doppler; NIRS, near-infrared spectroscopy; vmean, mean blood velocity from one cardiac cycle; vmax, maximal velocity/flow from one cardiac cycle; vmin, minimum velocity/flow from one cardiac cycle; CVC, cerebrovascular conductance; MAP, mean arterial pressure; CVR, cerebrovascular resistance; RAP, resistance area product; CCP, critical closing pressure; PI, pulsatility index; PR, pulsatility ratio.

[a]Beat-by-beat blood pressure can be recorded from a variety of available devices including finometer, intra-arterial pressure, etc. *Lateralization* refers to the difference in hyperemic responses between the left and right hemispheres, which is calculated by relative percent change (left vs. right). Essentially, any permutation of the above variables can be calculated.

hyperemia contours for presentation. The use of an approach such as this would serve to standardize the field interested in human neurovascular coupling, increase sensitivity of studies in laboratories currently limited to rudimentary peak responses, and provide a platform for between-laboratory comparisons. The software can be used with data collected on any charting software where data extraction can occur on a beat-by-beat basis and should ideally be gated by the QRS component of the ECG. Furthermore, this software merges with breath-by-breath $PETCO_2$ values. Beat-by-beat, and breath-by-breath data is cubic spline interpolated at 5 Hz to generate a single contour for cycles of stimulus on/off tasks (i.e., eyes-open/closed). Once interpolated and re-sampled, this software then calculates a number of metrics such as conductance, normalized to changes in $PETCO_2$ on a beat-by-beat basis. A list of the key metrics that can be obtained, and the various time-bins are outlined in Table 2. Furthermore, the mathematical formulas and theoretical physiological underpinnings are presented in Table 2.

Conclusions

Neurovascular coupling is a critical component of CBF regulation, having implications for cerebrovascular, autonomic, and cognitive dysfunction. Detailed knowledge has been accumulated related to neurovascular coupling *in vitro*, or in non-human models that unfortunately suffer from non-physiological approaches and/or unintended secondary consequences of vasoactive sedatives/anaesthetics. We are at an embryonic stage regarding neurovascular coupling function using an *in vivo* human model. One primary reason for this lack of development is inappropriate and inconsistent analysis strategies and stimulation paradigms.

A major concern related to neurovascular coupling is the lack of association with primary risk factors and relatively small sample sizes in clinical studies. This is due partially to the extremely time-consuming manual data analysis required for each individual in a study. In order to progress beyond this issue, a streamlined analysis using standardized software is needed to allow for large data set incorporation with associated risk-factor prediction for neurovascular coupling impairment within healthy and clinical populations, as well as across the life-span. Further, more studies will be able to develop an adjunct and clinically relevant cerebrovascular outcome measure when evaluating therapeutic interventions; with the capacity to impact management strategies for a number of risk factors and clinical conditions. It is our vision that a widespread implementation and utilization of standardized software would rapidly progress the field and benefit our understanding of neurovascular coupling.

Funding

A.A.P. is a Research Fellow and Postdoctoral Fellow funded by the Craig H. Neilsen Foundation, the Heart and Stroke Foundation of Canada (Focus on Stroke), and Michael Smith Foundation for Health Research. M.M.Z. is funded by Canadian Institute for Health Research (Scholarship). A.V.K. is funded by a Chair in Rehabilitation Medicine, the Canadian Institute for Health Research (Team Grant), Rick Hansen Foundation Clinical Outcome Measures and Optimizing Neurorecovery Program, the Craig Neilson Foundation, Christopher and Dana Reeves Foundation, and the Heart and Stroke Foundation of Canada. P.N.A. is supported by a Canada Research Chair in Cerebrovascular Physiology and Natural Sciences and Engineering Research Council (Canada) Discovery Grant.

Declaration of conflicting interests

The author(s) declared no potential conflicts of interest with respect to the research, authorship, and/or publication of this article.

Authors' contributions

Aaron A. Phillips – Conception and design, drafting and editing manuscript; Franco Chan – Conception and design, drafting and editing manuscript; Mei Mu Zi Zheng – Conception and design, drafting and editing manuscript; Andrei V. Krassioukov – Conception and design, editing manuscript; Philip N. Ainslie – Conception and design, drafting and editing manuscript. All authors provided final approval of the present version for publication. Our proposed software is openly accessible for assessments, testing and further development by contacting Dr. Aaron Phillips: aaphill@interchange.ubc.ca

References

1. Dienel GA and Hertz L. Glucose and lactate metabolism during brain activation. *J Neurosci Res* 2001; 66: 824–838.
2. Attwell D, Buchan AM, Charpak S, et al. Glial and neuronal control of brain blood flow. *Nature* 2010; 468: 232–243.
3. Mulligan SJ and MacVicar BA. Calcium transients in astrocyte endfeet cause cerebrovascular constrictions. *Nature* 2004; 431: 195–199.
4. Hamel E. Perivascular nerves and the regulation of cerebrovascular tone. *J Appl Physiol* 2006; 100: 1059–1064.
5. Lincoln J. Innervation of cerebral arteries by nerves containing 5-hydroxytryptamine and noradrenaline. *Pharmacol Ther* 1995; 68: 473–501.
6. Cipolla MJ, Li R and Vitullo L. Perivascular innervation of penetrating brain parenchymal arterioles. *J Cardiovasc Pharmacol* 2004; 44: 1–8.
7. Paulson OB, Strandgaard S and Edvinsson L. Cerebral autoregulation. *Cerebrovasc Brain Metab Rev* 1990; 2: 161.
8. Phillips AA, Ainslie PN, Krassioukov AV, et al. Regulation of cerebral blood flow after spinal cord injury. *J Neurotrauma* 2013; 30: 1551–1563.

9. Willie CK, Tzeng Y-C, Fisher JA, et al. Integrative regulation of human brain blood flow. *J Physiol* 2014; doi:10.1113/jphysiol.2013.268953.
10. Aaslid R, Lindegaard K-FF, Sorteberg W, et al. Cerebral autoregulation dynamics in humans. *Stroke* 1989; 20: 45–52.
11. Heistad DD, Marcus ML and Gross PM. Effects of sympathetic nerves on cerebral vessels in dog, cat, and monkey. *Am J Physiol* 1978; 235: H544–H552.
12. Faraci FM, Heistad DD and Mayhan WG. Role of large arteries in regulation of blood flow to brain stem in cats. *J Physiol* 1987; 387: 115–123.
13. Faraci FM, Mayhan WG and Heistad DD. Segmental vascular responses to acute hypertension in cerebrum and brain stem. *Am J Physiol* 1987; 252: H738–H742.
14. Willie CK, Macleod DB, Shaw AD, et al. Regional brain blood flow in man during acute changes in arterial blood gases. *J Physiol* 2012; 590: 3261–3275.
15. Lewis NC, Smith KJ, Bain AR, et al. Impact of transient hypotension on regional cerebral blood flow in humans. *Clin Sci (London)* 2015; doi:10.1042/CS20140751.
16. Edvinsson L. Characterization of the contractile effect of neuropeptide Y in feline cerebral arteries. *Acta Physiol Scand* 1985; 125: 33–41.
17. Edvinsson L. Neurogenic mechanisms in the cerebrovascular bed. Autonomic nerves, amine receptors and their effects on cerebral blood flow. *Acta Physiol Scand Suppl* 1975; 427: 1.
18. Bleys RL, Cowen T, Groen GJ, et al. Perivascular nerves of the human basal cerebral arteries: I. Topographical distribution. *J Cereb Blood Flow Metab* 1996; 16: 1034–1047.
19. Sercombe R, Aubineau P, Edvinsson L, et al. Neurogenic influence on local cerebral blood flow. effect of catecholamines or sympathetic stimulation as correlated with the sympathetic innervation. *Neurology* 1975; 25: 954–963.
20. *Cerebral blood flow and metabolism*. Lippincott Williams & Wilkins, 2002.
21. Zhang R, Zuckerman JH, Iwasaki K, et al. Autonomic neural control of dynamic cerebral autoregulation in humans. *Circulation* 2002; 106: 1814–1820.
22. Hamner JW, Tan CO, Lee K, et al. Sympathetic control of the cerebral vasculature in humans. *Stroke* 2010; 41: 102–109.
23. Ogoh S, Brothers RM, Eubank WL, et al. Autonomic neural control of the cerebral vasculature: acute hypotension. *Stroke* 2008; 39: 1979–1987.
24. Hamner JW, Tan CO, Tzeng Y-CC, et al. Cholinergic control of the cerebral vasculature in humans. *J Physiol* 2012; 590: 6343–6352.
25. Donders FC. Die Bewegungen des Gehirns und die Veränderungen der Gefässfüllung der Pia mater. *Schmid's Fahrbucher* 1851; 69: 16–20.
26. Mosso A. Sulla circolazione del cervello dell'uomo. *Atti R Accad Lincei* 1880; 5: 237–358.
27. Roy CS and Sherrington CS. On the regulation of the blood-supply of the brain. *J Physiol* 1890; 11: 85–158.17.
28. Iadecola C and Nedergaard M. Glial regulation of the cerebral microvasculature. *Nat Neurosci* 2007; 10: 1369–1376.
29. Lecrux C and Hamel E. The neurovascular unit in brain function and disease. *Acta Physiol (Oxf)* 2011; 203: 47–59.
30. Busija DW, Bari F, Domoki F, et al. Mechanisms involved in the cerebrovascular dilator effects of N-methyl-d-aspartate in cerebral cortex. *Brain Res Rev* 2007; 56: 89–100.
31. Ko KR, Ngai AC and Winn HR. Role of adenosine in regulation of regional cerebral blood flow in sensory cortex. *Am J Physiol* 1990; 259: H1703–H1708.
32. Porter JT and McCarthy KD. Hippocampal astrocytes in situ respond to glutamate released from synaptic terminals. *J Neurosci* 1996; 16: 5073–5081.
33. Gordon GRJ, Choi HB, Rungta RL, et al. Brain metabolism dictates the polarity of astrocyte control over arterioles. *Nature* 2008; 456: 745–749.
34. Cauli B, Tong X-K, Rancillac A, et al. Cortical GABA interneurons in neurovascular coupling: relays for subcortical vasoactive pathways. *J Neurosci* 2004; 24: 8940–8949.
35. Vaucher E, Tong XK, Cholet N, et al. GABA neurons provide a rich input to microvessels but not nitric oxide neurons in the rat cerebral cortex: a means for direct regulation of local cerebral blood flow. *J Comp Neurol* 2000; 421: 161–171.
36. Kawaguchi Y and Kubota Y. GABAergic cell subtypes and their synaptic connections in rat frontal cortex. *Cereb Cortex* 1997; 7: 476–486.
37. Lin A-L, Fox PT, Hardies J, et al. Nonlinear coupling between cerebral blood flow, oxygen consumption, and ATP production in human visual cortex. *Proc Natl Acad Sci USA* 2010; 107: 8446–8451.
38. Jespersen SN and Østergaard L. The roles of cerebral blood flow, capillary transit time heterogeneity, and oxygen tension in brain oxygenation and metabolism. *J Cereb Blood Flow Metab* 2012; 32: 264–277.
39. Schmithorst VJ, Vannest J, Lee G, et al. Evidence that neurovascular coupling underlying the BOLD effect increases with age during childhood. *Hum Brain Mapp* 2015; 36: 1–15.
40. Bonder DE and McCarthy KD. Astrocytic Gq-GPCR-linked IP3R-dependent Ca2+ signaling does not mediate neurovascular coupling in mouse visual cortex in vivo. *J Neurosci* 2014; 34: 13139–13150.
41. Rosenegger DG and Gordon GR. A Slow or Modulatory Role of Astrocytes in Neurovascular Coupling. *Microcirculation* 2015; doi:10.1111/micc.12184.
42. Tayebati SK, Tomassoni D and Amenta F. Spontaneously hypertensive rat as a model of vascular brain disorder: microanatomy, neurochemistry and behavior. *J Neurol Sci* 2012; 322: 241–249.
43. Shepro D and Morel NM. Pericyte physiology. *FASEB J* 1993; 7: 1031–8.
44. Puro DG. Physiology and pathobiology of the pericyte-containing retinal microvasculature: new developments. *Microcirculation* 2007; 14: 1–10.
45. Lovick TA, Brown LA and Key BJ. Neurovascular relationships in hippocampal slices: physiological and anatomical studies of mechanisms underlying flow-

metabolism coupling in intraparenchymal microvessels. *Neuroscience* 1999; 92: 47–60.
46. Peppiatt CM, Howarth C, Mobbs P, et al. Bidirectional control of CNS capillary diameter by pericytes. *Nature* 2006; 443: 700–704.
47. Lu K, Clark JW, Ghorbel FH, et al. Cerebral autoregulation and gas exchange studied using a human cardiopulmonary model. *Am J Physiol Heart Circ Physiol* 2004; 286: H584–H601.
48. Boas DA, Jones SR, Devor A, et al. A vascular anatomical network model of the spatio-temporal response to brain activation. *Neuroimage* 2008; 40: 1116–1129.
49. Pries AR, Secomb TW and Gaehtgens P. Biophysical aspects of blood flow in the microvasculature. *Cardiovasc Res* 1996; 32: 654–667.
50. Takano T, Tian G-F, Peng W, et al. Astrocyte-mediated control of cerebral blood flow. *Nat Neurosci* 2006; 9: 260–267.
51. Tran CHT and Gordon GR. Acute two-photon imaging of the neurovascular unit in the cortex of active mice. *Front Cell Neurosci* 2015; 9: 11.
52. Phillips AA, Warburton DE, Ainslie PN, et al. Regional neurovascular coupling and cognitive performance in those with low blood pressure secondary to high-level spinal cord injury: improved by alpha-1 agonist midodrine hydrochloride. *J Cereb Blood Flow Metab* 2014; 34: 794–801.
53. Salinet ASM, Robinson TG and Panerai RB. Active, passive, and motor imagery paradigms: component analysis to assess neurovascular coupling. *J Appl Physiol* 2013; 114: 1406–1412.
54. Maggio P, Salinet ASM, Robinson TG, et al. Influence of CO2 on neurovascular coupling: interaction with dynamic cerebral autoregulation and cerebrovascular reactivity. *Physiol Rep* 2014; 2: e00280.
55. Willie CK, Cowan EC, Ainslie PN, et al. Neurovascular coupling and distribution of cerebral blood flow during exercise. *J Neurosci Methods* 2011; 198: 270–273.
56. Girouard H and Iadecola C. Neurovascular coupling in the normal brain and in hypertension, stroke, and Alzheimer disease. *J Appl Physiol* 2006; 100: 328–335.
57. Janzarik WG, Ehmann R, Ehlers E, et al. Neurovascular coupling in pregnancy and the risk of preeclampsia. *Stroke* 2014; 45: 2792–2794.
58. Gommer ED, Bogaarts G, Martens EGHJ, et al. Visually evoked blood flow responses and interaction with dynamic cerebral autoregulation: correction for blood pressure variation. *Med Eng Phys* 2014; 36: 613–619.
59. Flück D, Beaudin AE, Steinback CD, et al. Effects of aging on the association between cerebrovascular responses to visual stimulation, hypercapnia and arterial stiffness. *Front Physiol* 2014; 5: 49–60.
60. Noonan JE, Dusting GJ, Nguyen TT, et al. Flicker light-induced retinal vasodilation is unaffected by inhibition of epoxyeicosatrienoic acids and prostaglandins in humans. *Invest Ophthalmol Vis Sci* 2014; 55: 7007–7013.
61. Stewart JM, Del Pozzi AT, Pandey A, et al. Oscillatory cerebral blood flow is associated with impaired neurocognition and functional hyperemia in postural tachycardia syndrome during graded tilt. *Hypertension* 2015; 65: 636–643.
62. Zhang N, Liu Z, He B, et al. Noninvasive study of neurovascular coupling during graded neuronal suppression. *J Cereb Blood Flow Metab* 2008; 28: 280–290.
63. Rosengarten B, Huwendiek O and Kaps M. Neurovascular coupling and cerebral autoregulation can be described in terms of a control system. *Ultrasound Med Biol* 2001; 27: 189–193.
64. Phillips AA, Smith KJ, Zheng MM, et al. Volumetric neurovascular coupling in man: the effect of cerebrovascular L-type calcium channel blockade. *J Appl Physiol*.
65. Chacon M, Araya C and Panerai RB. Non-linear multivariate modeling of cerebral hemodynamics with autoregressive support vector machines. *Med Eng Phys* 2011; 33: 180–187.
66. Moody M, Panerai RB, Eames PJ, et al. Cerebral and systemic hemodynamic changes during cognitive and motor activation paradigms. *Am J Physiol Regul Integr Comp Physiol* 2005; 288: R1581–R1588.
67. Maggio P, Salinet ASM, Panerai RB, et al. Does hypercapnia-induced impairment of cerebral autoregulation affect neurovascular coupling? a functional TCD study. *J Appl Physiol* 2013; 115: 491–497.
68. Ances BM, Greenberg JH and Detre JA. The effects of graded hypercapnia on the activation flow coupling response due to forepaw stimulation in alpha-chloralose anesthetized rats. *Brain Res* 2001; 911: 82–88.
69. Blicher JU, Stagg CJ, O'Shea J, et al. Visualization of altered neurovascular coupling in chronic stroke patients using multimodal functional MRI. *J Cereb Blood Flow Metab* 2012; 32: 2044–2054.
70. Bundo M, Inao S, Nakamura A, et al. Changes of neural activity correlate with the severity of cortical ischemia in patients with unilateral major cerebral artery occlusion. *Stroke* 2002; 33: 61–66.
71. Duschek S and Schandry R. Cognitive performance and cerebral blood flow in essential hypotension. *Psychophysiology* 2004; 41: 905–913.
72. Duschek S and Schandry R. Reduced brain perfusion and cognitive performance due to constitutional hypotension. *Clin Auton Res* 2007; 17: 69–76.
73. Azevedo E, Castro P, Santos R, et al. Autonomic dysfunction affects cerebral neurovascular coupling. *Clin Auton Res* 2011; 21: 395–403.
74. Salinet ASM, Robinson TG and Panerai RB. Cerebral blood flow response to neural activation after acute ischemic stroke: a failure of myogenic regulation? *J Neurol* 2013; 260: 2588–2595.
75. Brouns R and De Deyn PP. The complexity of neurobiological processes in acute ischemic stroke. *Clin Neurol Neurosurg* 2009; 111: 483–495.
76. Østergaard L, Engedal TS, Aamand R, et al. Capillary transit time heterogeneity and flow-metabolism coupling after traumatic brain injury. *J Cereb Blood Flow Metab* 2014; 34: 1585–1598.
77. Hinzman JM, Andaluz N, Shutter LA, et al. Inverse neurovascular coupling to cortical spreading depolarizations in severe brain trauma. *Brain* 2014; 137: 2960–2972.

78. Lok J, Wang X-S, Xing CH, et al. Targeting the neurovascular unit in brain trauma. *CNS Neurosci Ther* 2014; doi:10.1111/cns.12359.
79. Guiney H, Lucas SJ, Cotter JD, et al. Evidence cerebral blood-flow regulation mediates exercise-cognition links in healthy young adults. *Neuropsychology* 2015; 29: 1–9.
80. Jegede AB, Rosado-Rivera D, Bauman WA, et al. Cognitive performance in hypotensive persons with spinal cord injury. *Clin Auton Res* 2010; 20: 3–9.
81. Duschek S, Hadjamu M and Schandry R. Enhancement of cerebral blood flow and cognitive performance following pharmacological blood pressure elevation in chronic hypotension. *Psychophysiology* 2007; 44: 145–53.
82. Boms N, Yonai Y, Molnar S, et al. Effect of smoking cessation on visually evoked cerebral blood flow response in healthy volunteers. *J Vasc Res* 2010; 47: 214–220.
83. Sekhon MS, Griesdale DE, Czosnyka M, et al. The effect of red blood cell transfusion on cerebral autoregulation in patients with severe traumatic brain injury. *Neurocrit Care* 2015; 23: 210–216.
84. Coverdale NS, Gati JS, Opalevych O, et al. Cerebral blood flow velocity underestimates cerebral blood flow during modest hypercapnia and hypocapnia. *J Appl Physiol*2014; jap.00285.2014.
85. Aaslid R. Visually evoked dynamic blood flow response of the human cerebral circulation. *Stroke* 1987; 18: 771–775.
86. Azevedo E, Santos R, Freitas J, et al. Deep brain stimulation does not change neurovascular coupling in non-motor visual cortex: an autonomic and visual evoked blood flow velocity response study. *Parkinsonism Relat Disord* 2010; 16: 600–603.
87. Silvestrini M, Caltagirone C, Cupini LM, et al. Activation of healthy hemisphere in poststroke recovery. a transcranial Doppler study. *Stroke* 1993; 24: 1673–1677.
88. Klingelhöfer J, Matzander G, Sander D, et al. Assessment of functional hemispheric asymmetry by bilateral simultaneous cerebral blood flow velocity monitoring. *J Cereb Blood Flow Metab* 1997; 17: 577–585.
89. Phillips AA, Krassioukov AV, Ainslie PN, et al. Perturbed and spontaneous regional cerebral blood flow responses to changes in blood pressure after high level spinal cord injury: the effect of midodrine. *J Appl Physiol* 2014; 116: 645–653.
90. Phillips AA, Warburton DE, Ainslie PN, et al. Dynamic cerebral blood flow regulation in those with schizophrenia. *Unpubl Find*2015.
91. Willie CK, Colino FL, Bailey DM, et al. Utility of transcranial Doppler ultrasound for the integrative assessment of cerebrovascular function. *J Neurosci Methods* 2011; 196: 221–237.
92. Yonai Y, Boms N, Molnar S, et al. Acetazolamide-induced vasodilation does not inhibit the visually evoked flow response. *J Cereb Blood Flow Metab* 2010; 30: 516–521.
93. Rosengarten B, Auch D and Kaps M. Effects of initiation and acute withdrawal of statins on the neurovascular coupling mechanism in healthy, normocholesterolemic humans. *Stroke* 2007; 38: 3193–3197.
94. Aaslid R. *Transcranial Doppler sonography*. Springer Verlag: New York, 1987.
95. Purkayastha S and Sorond F. Transcranial Doppler ultrasound: technique and application. *Semin Neurol* 2012; 32: 411–420.
96. Verbree J, Bronzwaer A-SGT, Ghariq E, et al. Assessment of middle cerebral artery diameter during hypocapnia and hypercapnia in humans using ultra-high-field MRI. *J Appl Physiol* 2014; 117: 1084–1089.
97. Ainslie PN and Hoiland RL. Transcranial Doppler ultrasound: valid, invalid, or both? *J Appl Physiol* 2014; 117: 1081–1083.
98. Salinet ASM, Robinson TG and Panerai RB. Effects of cerebral ischemia on human neurovascular coupling, CO2 reactivity, and dynamic cerebral autoregulation. *J Appl Physiol* 2015; 118: 170–177.
99. Jasdzewski G, Strangman G, Wagner J, et al. Differences in the hemodynamic response to event-related motor and visual paradigms as measured by near-infrared spectroscopy. *Neuroimage* 2003; 20: 479–488.
100. Dutta A, Jacob A, Chowdhury SR, et al. EEG-NIRS based assessment of neurovascular coupling during anodal transcranial direct current stimulation – a stroke case series. *J Med Syst* 2015; 39: 205.
101. Mackert B-M, Wübbeler G, Leistner S, et al. Neurovascular coupling analyzed non-invasively in the human brain. *Neuroreport* 2004; 15: 63–66.
102. Mackert B-M, Leistner S, Sander T, et al. Dynamics of cortical neurovascular coupling analyzed by simultaneous DC-magnetoencephalography and time-resolved near-infrared spectroscopy. *Neuroimage* 2008; 39: 979–986.
103. Ferrari M and Quaresima V. A brief review on the history of human functional near-infrared spectroscopy (fNIRS) development and fields of application. *Neuroimage* 2012; 63: 921–935.
104. Kimoto H, Ohno T, Takashima S, et al. The effect of acetazolamide and carbon dioxide on cerebral hemodynamic changes on near-infrared spectroscopy in young rabbits. *Brain Dev* 17: 261–263.
105. Strait M and Scheutz M. What we can and cannot (yet) do with functional near infrared spectroscopy. *Front Neurosci* 2014; 8: 117.
106. Cui X, Bray S, Bryant DM, et al. A quantitative comparison of NIRS and fMRI across multiple cognitive tasks. *Neuroimage* 2011; 54: 2808–2821.
107. Van Beek AHEA, Lagro J, Olde-Rikkert MGM, et al. Oscillations in cerebral blood flow and cortical oxygenation in Alzheimer's disease. *Neurobiol Aging* 2012; 33428.e21–31.
108. Vernieri F, Tibuzzi F, Pasqualetti P, et al. Increased cerebral vasomotor reactivity in migraine with aura: an autoregulation disorder? A transcranial Doppler

and near-infrared spectroscopy study. *Cephalalgia* 2008; 28: 689–695.
109. Palazzo P, Tibuzzi F, Pasqualetti P, et al. Is there a role of near-infrared spectroscopy in predicting the outcome of patients with carotid artery occlusion? *J Neurol Sci* 2010; 292: 36–39.
110. Szabo K, Lako E, Juhasz T, et al. Hypocapnia induced vasoconstriction significantly inhibits the neurovascular coupling in humans. *J Neurol Sci* 2011; 309: 58–62.
111. Yamaguchi Y, Ikemura T, Kashima H, et al. Effects of vasodilatation and pressor response on neurovascular coupling during dynamic exercise. *Eur J Appl Physiol* 2015; 115: 619–625.
112. Fabjan A, Bajrović FF, Musizza B, et al. Study of neurovascular coupling during cold pressor test in patients with migraine. *Cephalalgia*2014; doi:10.1177/0333102414554661.
113. Schöning M, Walter J and Scheel P. Estimation of cerebral blood flow through color duplex sonography of the carotid and vertebral arteries in healthy adults. *Stroke* 1994; 25: 17–22.
114. Jones H, Lewis NCS, Thompson A, et al. Diurnal variation in vascular function: role of sleep. *Chronobiol Int* 2012; 29: 271–277.
115. Adkisson EJ, Casey DP, Beck DT, et al. Central, peripheral and resistance arterial reactivity: fluctuates during the phases of the menstrual cycle. *Exp Biol Med (Maywood)* 2010; 235: 111–118.
116. Tyldum GA, Schjerve IE, Tjønna AE, et al. Endothelial dysfunction induced by post-prandial lipemia: complete protection afforded by high-intensity aerobic interval exercise. *J Am Coll Cardiol* 2009; 53: 200–206.
117. Lavi T, Karasik A, Koren-Morag N, et al. The acute effect of various glycemic index dietary carbohydrates on endothelial function in nondiabetic overweight and obese subjects. *J Am Coll Cardiol* 2009; 53: 2283–2287.
118. Hijmering ML, de Lange DW, Lorsheyd A, et al. Binge drinking causes endothelial dysfunction, which is not prevented by wine polyphenols: a small trial in healthy volunteers. *Neth J Med* 2007; 65: 29–35.
119. Papamichael CM, Aznaouridis KA, Karatzis EN, et al. Effect of coffee on endothelial function in healthy subjects: the role of caffeine. *Clin Sci (London)* 2005; 109: 55–60.
120. Dawson EA, Whyte GP, Black MA, et al. Changes in vascular and cardiac function after prolonged strenuous exercise in humans. *J Appl Physiol* 2008; 105: 1562–1568.
121. Tinken TM, Thijssen DHJ, Black MA, et al. Time course of change in vasodilator function and capacity in response to exercise training in humans. *J Physiol* 2008; 586: 5003–5012.
122. Rognmo O, Bjørnstad TH, Kahrs C, et al. Endothelial function in highly endurance-trained men: effects of acute exercise. *J Strength Cond Res* 2008; 22: 535–542.
123. Harris RA, Nishiyama SK, Wray DW, et al. The effect of oral antioxidants on brachial artery flow-mediated dilation following 5 and 10 min of ischemia. *Eur J Appl Physiol* 2009; 107: 445–453.
124. Taneva E, Borucki K, Wiens L, et al. Early effects on endothelial function of atorvastatin 40 mg twice daily and its withdrawal. *Am J Cardiol* 2006; 97: 1002–1006.
125. Otto ME, Svatikova A, Barretto RB de M, et al. Early morning attenuation of endothelial function in healthy humans. *Circulation* 2004; 109: 2507–2510.
126. Fan J-L, Burgess KR, Thomas KN, et al. Influence of indomethacin on ventilatory and cerebrovascular responsiveness to CO2 and breathing stability: the influence of PCO2 gradients. *Am J Physiol Regul Integr Comp Physiol* 2010; 298: R1648–R1658.
127. Markus HS, Vallance P and Brown MM. Differential effect of three cyclooxygenase inhibitors on human cerebral blood flow velocity and carbon dioxide reactivity. *Stroke* 1994; 25: 1760–1764.
128. Davis RJ, Murdoch CE, Ali M, et al. EP4 prostanoid receptor-mediated vasodilatation of human middle cerebral arteries. *Br J Pharmacol* 2004; 141: 580–585.
129. Metea MR and Newman EA. Glial cells dilate and constrict blood vessels: a mechanism of neurovascular coupling. *J Neurosci* 2006; 26: 2862–2870.
130. Zonta M, Angulo MC, Gobbo S, et al. Neuron-to-astrocyte signaling is central to the dynamic control of brain microcirculation. *Nat Neurosci* 2003; 6: 43–50.
131. Armstead WM. Role of ATP-sensitive K+ channels in cGMP-mediated pial artery vasodilation. *Am J Physiol* 1996; 270: H423–H426.
132. Harder DR, Lange AR, Gebremedhin D, et al. Cytochrome P450 metabolites of arachidonic acid as intracellular signaling molecules in vascular tissue. *J Vasc Res* 34: 237–243.
133. Roman RJ. P-450 metabolites of arachidonic acid in the control of cardiovascular function. *Physiol Rev* 2002; 82: 131–185.
134. De Silva TM and Faraci FM. Effects of angiotensin II on the cerebral circulation: role of oxidative stress. *Front Physiol* 2013; 3: 484.
135. Takeda S, Sato N, Takeuchi D, et al. Angiotensin receptor blocker prevented beta-amyloid-induced cognitive impairment associated with recovery of neurovascular coupling. *Hypertension* 2009; 54: 1345–1352.
136. Nicolakakis N and Hamel E. Neurovascular function in Alzheimer's disease patients and experimental models. *J Cereb Blood Flow Metab* 2011; 31: 1354–1370.
137. Chow N, Bell RD, Deane R, et al. Serum response factor and myocardin mediate arterial hypercontractility and cerebral blood flow dysregulation in Alzheimer's phenotype. *Proc Natl Acad Sci USA* 2007; 104: 823–828.
138. Zlokovic BV. Neurovascular mechanisms of Alzheimer's neurodegeneration. *Trends Neurosci* 2005; 28: 202–208.
139. Vetri F, Xu H, Paisansathan C, et al. Impairment of neurovascular coupling in type 1 diabetes mellitus in rats is linked to PKC modulation of BK(Ca) and Kir channels. *Am J Physiol Heart Circ Physiol* 2012; 302: H1274–H1284.
140. Gandhi GK, Ball KK, Cruz NF, et al. Hyperglycaemia and diabetes impair gap junctional communication among astrocytes. *ASN Neuro* 2010; 2: e00030.

141. Davenport MH, Hogan DB, Eskes GA, et al. Cerebrovascular reserve: the link between fitness and cognitive function? *Exerc Sport Sci Rev* 2012; 40: 153–158.
142. Bracco L, Bessi V, Alari F, et al. Cerebral hemodynamic lateralization during memory tasks as assessed by functional transcranial Doppler (fTCD) sonography: effects of gender and healthy aging. *Cortex* 2011; 47: 750–758.
143. O'Leary DS. Regional vascular resistance vs conductance: which index for baroreflex responses? *Am J Physiol* 1991; 260: H632–H637.
144. Claassen JAHR, Zhang R, Fu Q, et al. Transcranial Doppler estimation of cerebral blood flow and cerebrovascular conductance during modified rebreathing. *J Appl Physiol* 2007; 102: 870–877.
145. Panerai RB, Salinet ASM, Brodie FG, et al. The influence of calculation method on estimates of cerebral critical closing pressure. *Physiol Meas* 2011; 32: 467–482.
146. Robertson AD, Edgell H and Hughson RL. Assessing cerebrovascular autoregulation from critical closing pressure and resistance area product during upright posture in aging and hypertension. *Am J Physiol Heart Circ Physiol* 2014; 307: H124–H133.
147. Panerai RB. The critical closing pressure of the cerebral circulation. *Med Eng Phys* 2003; 25: 621–632.
148. Woodcock JP, Gosling RG and Fitzgerald DE. A new noninvasive technique for assessment of superficial femoral artery obstruction. *Br J Surg* 1972; 59: 226–231.
149. Levine BD, Giller CA, Lane LD, et al. Cerebral versus systemic hemodynamics during graded orthostatic stress in humans. *Circulation* 1994; 90: 298–306.